

*This copy is for your personal, non-commercial use only.*

**If you wish to distribute this article to others**, you can order high-quality copies for your colleagues, clients, or customers by [clicking here](#).

**Permission to republish or repurpose articles or portions of articles** can be obtained by following the guidelines [here](#).

***The following resources related to this article are available online at [www.sciencemag.org](http://www.sciencemag.org) (this information is current as of June 7, 2010 ):***

**Updated information and services**, including high-resolution figures, can be found in the online version of this article at:

<http://www.sciencemag.org/cgi/content/full/291/5503/451>

This article **cites 27 articles**, 4 of which can be accessed for free:

<http://www.sciencemag.org/cgi/content/full/291/5503/451#otherarticles>

This article has been **cited by** 373 article(s) on the ISI Web of Science.

This article has been **cited by** 2 articles hosted by HighWire Press; see:

<http://www.sciencemag.org/cgi/content/full/291/5503/451#otherarticles>

This article appears in the following **subject collections**:

Physics

<http://www.sciencemag.org/cgi/collection/physics>

# Coupling and Entangling of Quantum States in Quantum Dot Molecules

M. Bayer,<sup>1\*</sup> P. Hawrylak,<sup>2\*</sup> K. Hinzer,<sup>2,3</sup> S. Fafard,<sup>2</sup> M. Korkusinski,<sup>2,3</sup> Z. R. Wasilewski,<sup>2</sup> O. Stern,<sup>1</sup> A. Forchel<sup>1</sup>

We demonstrate coupling and entangling of quantum states in a pair of vertically aligned, self-assembled quantum dots by studying the emission of an interacting electron-hole pair (exciton) in a single dot molecule as a function of the separation between the dots. An interaction-induced energy splitting of the exciton is observed that exceeds 30 millielectron volts for a dot layer separation of 4 nanometers. The results are interpreted by mapping the tunneling of a particle in a double dot to the problem of a single spin. The electron-hole complex is shown to be equivalent to entangled states of two interacting spins.

There is significant interest in quantum information processing using quantum dots (QDs) (1–8). The key building block of a quantum processor is a quantum gate, which is used to entangle the states of two quantum bits (qubits). Quantum gates have been realized using, e.g., ions in traps (9) and nuclear spins in molecules (10). We have recently proposed to use a pair of vertically aligned semiconductor QDs (shown schematically in Fig. 1A) as the optically driven solid state quantum gate (11), in which an electric field applied along the growth direction can localize individual carriers on the upper dot (index zero) or the lower dot (index one). The two different dot indices play the same role as the two states of a “spin” (a qubit) and are referred to as “isospin” (12). When the electric field is turned off, the quantum mechanical tunneling rotates the “isospin” leading to the superposition of two QD states. The quantum gate is built when two different particles, an electron and a hole, are created optically. In the presence of the electric field, the particles are localized on opposite dots. After switching off the electric field, the tunneling and interaction between the two particles should lead to the formation of entangled states. The states can be disentangled at a later time by preventing tunneling through the application of an electric field.

We present results which support the feasibility of this proposal. The first and crucial task is to demonstrate that a pair of vertically aligned self-assembled QDs with a controlled

geometry can be constructed. The second is to demonstrate that electrons (holes) tunnel coherently from dot  $|0\rangle$  to dot  $|1\rangle$ . The third task is to show that the tunneling indeed leads to entangled states of electron-hole pairs. The final task, the demonstration that one can put contacts on a single pair of dots and apply a vertical electric field to entangle/disentangle states is a technical challenge which can be tackled only after the first three tasks have successfully been accomplished. In this work, we isolate a single pair of vertically coupled quantum disks, inject electron-hole pairs, and study the evolution of their recombination spectrum as a function of the vertical separation between the dots. The dependence of the emission spectrum on the dot separation  $d$  is used to demonstrate the coherent tunneling of electrons and holes and the formation of entangled states, which we relate to the quantum information properties of the system.

Previous experimental (13–19) and theoretical (12, 20, 21) work on coupled QDs reported maximum coupling induced splittings of  $\sim 1$  meV resulting in a large sensitivity to thermal perturbations. These struc-

tures are therefore not very well suited for application to quantum information processing. In Stranski-Krastanow epitaxy (22–28), vertical self-alignment of QDs occurs because the strain field of a dot in a first layer facilitates the growth of a second dot above it. Here, this technique has been modified by an indium-flush procedure (29) to grow in close proximity two layers of vertically correlated InAs QDs separated by GaAs barriers. Each dot can be approximated by a disk with radius  $R$  and height  $h$  (Fig. 1A). The transmission electron microscope (TEM) picture (30) (Fig. 1B) shows such a QD molecule with a barrier of width  $d = 4$  nm measured from wetting layer to wetting layer. The typical dot height  $h$  is estimated to be between 1 and 2 nm and the typical radius  $R$  varies from 8 to 12 nm. The electronic states with orbital angular momentum  $m = 0, \pm 1, \dots$  in each disk can be characterized by the isospin (dot) index  $i = 0$  or  $i = 1$  (12).

For weak tunneling and strong lateral quantization, the basic physics is well described by a simple model of  $m = 0$  s-orbitals in each dot. There are two electron s-states  $|0\rangle$  and  $|1\rangle$  with energy  $E_s$  corresponding to dot “0” and “1”. As  $h \ll R$ , the wave function of a carrier in a disk is well localized along the growth direction. The Hamiltonian  $H$  in this basis

$$\begin{bmatrix} E_s & -t \\ -t & E_s \end{bmatrix} \quad (1)$$

is that of a spin in a perpendicular magnetic field. An electron tunnels from dot 0 to dot 1 with a tunneling probability  $\langle 0|H|1\rangle = t$  without changing angular momentum. The tunneling can be eliminated by a rotation to a set of symmetric (+) and antisymmetric (–) orbitals, which are linear superpositions of the isospin states (0,1)

$$\begin{bmatrix} |+\rangle \\ |-\rangle \end{bmatrix} = \frac{1}{\sqrt{2}} \begin{bmatrix} |0\rangle + |1\rangle \\ |0\rangle - |1\rangle \end{bmatrix} \quad (2)$$

The Hamiltonian in this basis is diagonal,

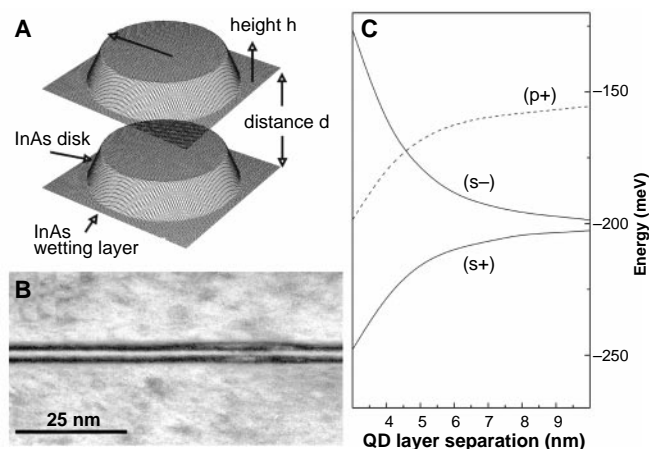


**Fig. 1.** (A) Schematic picture of a QD molecule. (B) TEM image of coupled InAs QDs separated by a GaAs barrier with 4-nm thickness. (C) Energies of the low-lying electron levels in a QD molecule as function of the separation between the dots.

<sup>1</sup>Physikalisches Institut, Universität Würzburg, Am Hubland, D-97074 Würzburg, Germany. <sup>2</sup>Institute for Microstructural Sciences, National Research Council, Ottawa, K1A 0R6, Canada. <sup>3</sup>Physics Department, University of Ottawa, Ottawa, Ontario, K1N 6N5, Canada.

\*To whom correspondence should be addressed. E-mail: mbayer@physik.uni-wuerzburg.de (M.B.); pawel.hawrylak@nrc.ca (P.H.)

with  $2t$  being the splitting (“Zeeman energy”) of the (+) and (−) levels. We show the results (Fig. 1C) of a calculation of the electron energies in a QD molecule versus barrier thickness for  $R = 8$  nm. The barrier height of the confinement potential is 800 meV, the effective electron mass is 0.043 (31, 32). From these calculations we expect a splitting of the s-shell which increases from  $\sim 5$  meV for  $d = 10$  nm to  $\sim 40$  meV for  $d = 4$  nm. For  $d = 4$  to 5 nm, a crossing of the antisymmetric s-state and the symmetric state from the p-shell with  $m = \pm 1$  is expected.

In a spectroscopic experiment we measure the recombination of an electron-hole complex, so that Coulomb correlations also need to be included. We now discuss a simple model of an exciton in a QD molecule in the weak tunneling limit. In Fig. 2A, we show the four isospin states of a single electron-hole pair:  $|0,0\rangle$ ,  $|1,1\rangle$ ,  $|0,1\rangle$ , and  $|1,0\rangle$ . The first two states correspond to an electron and a hole on dot “0” or dot “1” and can be created optically. The second pair corresponds to indirect electron-hole pairs, e.g., electron on dot “0” and hole on dot “1” and can only be created optically when there is a (small) overlap of the states on the two dots. The interband polarization operator  $P^+$  describing the creation of an electron-hole pair can be written as

$$P^+ |V\rangle = M_{00}[|0,0\rangle + |1,1\rangle] + M_{01}[|0,1\rangle + |1,0\rangle] \quad (3)$$

where the  $M_{ij} = \langle i|j\rangle$  are the overlap integrals

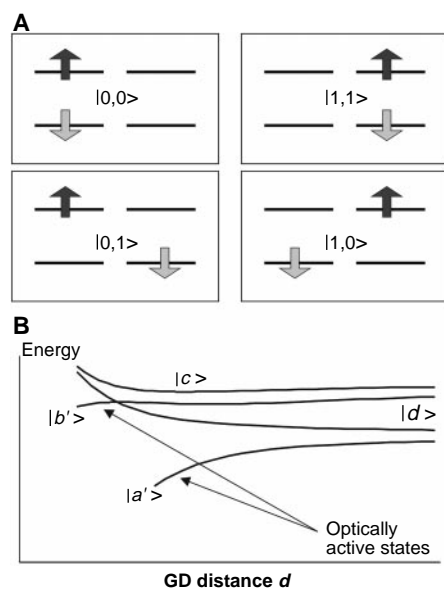


**Fig. 2.** (A) Scheme of the electron-hole pair configurations in a coupled pair of dots and their analogy to isospin configurations. In each panel, the left side corresponds to dot 0, the right side to dot 1. The dark arrows indicate the electron, the bright ones the hole. (B) Evolution of the entangled states of two coupled isospins (electron-hole pair) as function of the separation between the dots.

of the electron and hole wave functions on dots  $i$  and  $j$ . We therefore write the electron-hole pair states in a new basis of entangled states  $|a\rangle$ ,  $|b\rangle$ ,  $|c\rangle$ , and  $|d\rangle$  consistent with the interband polarization operator

$$\begin{bmatrix} |a\rangle \\ |b\rangle \\ |c\rangle \\ |d\rangle \end{bmatrix} = \frac{1}{\sqrt{2}} \begin{bmatrix} |0,0\rangle + |1,1\rangle \\ |0,1\rangle + |1,0\rangle \\ |0,1\rangle - |1,0\rangle \\ |0,0\rangle - |1,1\rangle \end{bmatrix} \quad (4)$$

Assuming for simplicity similar tunneling matrix elements for electron and hole, the electron-hole pair Hamiltonian in the basis ( $a$  through  $d$ ) is given by

$$\begin{pmatrix} E_x - (2M_0 + V_{01}^x) & -2(t + V_0) & 0 & 0 \\ -2(t + V_0) & E_x + (V_{00} - V_{01}^x) - (2M_0 + V_{01}^x) & 0 & 0 \\ 0 & 0 & E_x + (V_{00} - V_{01}^x) + (2M_0 + V_{01}^x) & 0 \\ 0 & 0 & 0 & E_x + (2M_0 + V_{01}^x) \end{pmatrix} \quad (5)$$

Here,  $E_x = 2E_s - V_{00}$  is the energy of an exciton on a single dot,  $-V_{00}$  is the electron-hole attraction for both particles being either on dot “0” or dot “1”,  $V_{01}^D$  is the direct interaction for an electron on dot 0 and a hole on dot 1,  $V_{01}^X$  is the matrix element for electron-hole pair scattering from dot 0 to dot 1, and  $V_0$  is the scattering matrix element involving only one particle, e.g.,  $\langle 00|V|01\rangle$ .

Only the optically active states  $|a\rangle$  and  $|b\rangle$  remain coupled via the tunneling matrix element  $t$ , which is renormalized by the Coulomb matrix elements  $V_{01}^X$  and  $V_0$ . The actual entangled eigenstates  $|a'\rangle$  and  $|b'\rangle$  of the exciton Hamiltonian are the excitonic analogs of the symmetric and antisymmetric single particle states, with the splitting controlled by

tunneling and by Coulomb interactions. The two entangled states  $|c\rangle$  and  $|d\rangle$  (the maximum entangled Bell state) are exact exciton eigenstates which are not coupled to the optically active states. They become addressable, e.g., through the optically active states  $|a'\rangle$  and  $|b'\rangle$  by infrared radiation.

The evolution of the four energy levels of the exciton as function of the dot separation is shown in Fig. 2B. When the dots are far apart, there are two groups of energy levels separated by the exciton binding energy  $V_{00}$ . When the dots are brought closer, the optically active states lower their energies and increase the

spacing in a manner similar to the symmetric-antisymmetric splitting of the single particle energy levels. The dark configurations separate from the bright ones and eventually are both located above the optically active ones. The key result is that the eigenstates  $a'$  and  $b'$  of the electron-hole Hamiltonian are a linear combination of the entangled states  $a$  and  $b$ . This guarantees that, for example, a state  $|10\rangle$  prepared by the application of an electric field will evolve into an entangled state once tunneling is allowed.

To demonstrate the validity of this model, photoluminescence spectroscopy was performed on single QD molecules to suppress inhomogeneous broadening of the emission (27, 28). For this purpose, lithographic tech-

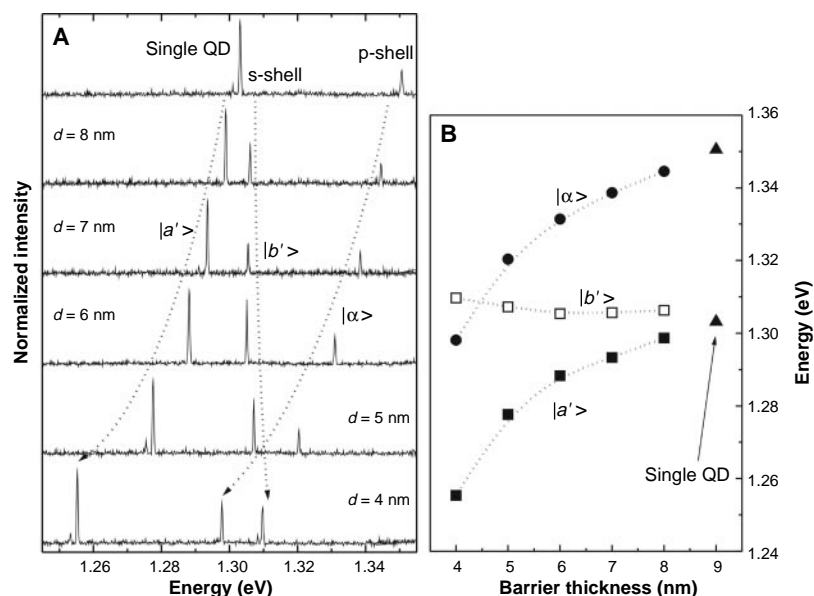


**Fig. 3.** (A) Emission spectra of single QD molecules at  $T \sim 60$  K for varying dot layer separation  $d$  from 8 down to 4 nm. As reference, also a single QD molecule was studied (top trace). (B) Evolution of the energies of emission lines in (A) as function of the distance between QD layers. Circles and squares denote experimental data, with dotted lines as guides to the eye.

niques were used to fabricate mesa structures, in which single dot molecules can be isolated due to the small lateral sizes ( $\sim 100$  nm) (33). The luminescence of single QD molecules, from which the evolution of the molecule states with decreasing dot separation (from top to bottom) is seen, is shown in Fig. 3A. The spectra were recorded at low excitation powers to avoid emission from multiexciton complexes. The temperature was  $\sim 60$  K so that not only ground state exciton emission, but also emission from excited exciton states is observed due to thermal excitation. In each case, symmetric single QD molecules were selected whose ground state emission is located at the center of the emission band of the corresponding arrays. The top trace in Fig. 3A shows the emission of a single QD which serves as reference for the emission from the QD molecules.

For a large dot separation  $d = 16$  nm in a molecule (34), two emission lines are observed in the s-shell with a splitting varying from 0 to 4 meV. For this distance and temperature, interaction with acoustical phonons prevents coherent tunneling, and we expect that the recombination takes place from either state  $|0,0\rangle$  or  $|1,1\rangle$  in individual QDs. The small splitting arises from dot inhomogeneities. For a dot separation  $d = 8$  nm, the s-shell emission splits into the entangled exciton states  $|a'\rangle$  and  $|b'\rangle$  (eigenstates of the electron-hole Hamiltonian). The energy splitting between them is about 10 meV. In addition, a further emission line denoted by  $|\alpha\rangle$  appears on the high energy side. The energies of all these features depend systematically on  $d$ : Reduction of the QD separation moves the emission line  $|a'\rangle$  strongly to lower energies, while the energy of the peak  $|b'\rangle$  is almost constant leading to an increase of their splitting to more than 25 meV. This behavior is suggestive of the energy level splitting due to the dot coupling. Hence we ascribe the two emission lines as originating from the entangled states of the s-shell exciton. The line  $|\alpha\rangle$ , on the other hand, moves to lower energies with decreasing  $d$  and can be assigned to the lowest entangled state from the p-shell.

The transition energies (summarized in Fig. 3B) show the dependence of exciton transition energies in the QD molecules in Fig. 3A versus wetting layer separation  $d$ . The observed behavior is in qualitative agreement with that expected from the model calculations in Fig. 2. Most importantly, the splitting between the optically active entangled exciton states of the s-shell is more than 30 meV when the barrier width becomes smaller than 5 nm. Despite the statistical variations, the observed trends, in particular for the energy splitting among the levels, are typical for the studied QD molecules.

References and Notes

1. C. H. Bennett, *Phys. Today* **48** (no. 10), 24 (1995).  
 2. D. P. DiVincenzo, *Science* **270**, 255 (1995).  
 3. A. Steane, *Rep. Prog. Phys.* **61**, 117 (1998).

4. G. Mahler, in *Information: New Questions to a Multidisciplinary Concept*, K. S. Kornwachs, K. Jacoby, Eds. (Akademie Verlag, Berlin, 1999), pp. 103–118.  
 5. A. Barenco, D. Deutsch, A. Ekert, R. Jozsa, *Phys. Rev. Lett.* **74**, 4083 (1995).  
 6. J. A. Brum, P. Hawrylak, *Superlattices Microstruct.* **22**, 431 (1997).  
 7. D. Loss, D. P. DiVincenzo, *Phys. Rev. A* **57**, 120 (1998).  
 8. P. Zanardi, F. Rossi, *Phys. Rev. Lett.* **81**, 4752 (1998).  
 9. C. A. Sackett et al., *Nature* **404**, 256 (2000).  
 10. I. L. Chuang, L. M. K. Vandersypen, X. Zhou, D. W. Leung, S. Lloyd, *Nature* **393**, 143 (1998).  
 11. P. Hawrylak, S. Fafard, Z. R. Wasilewski, *Condens. Matter News* **7**, 16 (1999).  
 12. J. J. Palacios, P. Hawrylak, *Phys. Rev. B* **51**, 1769 (1995).  
 13. R. H. Blick, D. Pfannkuche, R. J. Haug, K. von Klitzing, K. Eberl, *Phys. Rev. Lett.* **80**, 4032 (1998).  
 14. T. Fujisawa et al., *Science* **282**, 932 (1998).  
 15. L. Kouwenhoven, *Science* **268**, 1440 (1995).  
 16. G. Schedelbeck, W. Wegscheider, M. Bichler, G. Abstreiter, *Science* **278**, 1792 (1997).  
 17. D. G. Austing, T. Honda, K. Muraki, Y. Tokura, S. Tarucha, *Physica B* **249**, 206 (1998).  
 18. R. J. Luyken et al., *Nanotechnology* **10**, 14 (1999).  
 19. Y. Tokura, D. G. Austing, S. Tarucha, *J. Phys. Condens. Matter* **11**, 6023 (1999).  
 20. C. Pryor, *Phys. Rev. Lett.* **80**, 3579 (1998).  
 21. L. R. C. Fonseca, J. L. Jimenez, J. P. Leburton, *Phys. Rev. B* **58**, 9955 (1998).  
 22. L. Goldstein, F. Glas, J. Y. Marzin, M. N. Charasse, G. LeRoux, *Appl. Phys. Lett.* **47**, 1099 (1985).  
 23. P. R. Berger, K. Chang, P. Bhattacharya, J. Singh, K. K. Bajaj, *Appl. Phys. Lett.* **53**, 684 (1988).  
 24. Q. Xie, A. Madhukar, P. Chen, N. P. Kobayashi, *Phys. Rev. Lett.* **75**, 2542 (1995).  
 25. G. S. Solomon, J. A. Trezza, A. F. Marshall, J. J. S. Harris, *Phys. Rev. Lett.* **76**, 952 (1996).  
 26. S. Rouvimov et al., *J. Electron. Mater.* **27**, 427 (1998).  
 27. S. Fafard, M. Spanner, J. P. McCaffrey, Z. Wasilewski, *Appl. Phys. Lett.* **76**, 2707 (2000).  
 28. S. Fafard et al., *Phys. Rev. B* **59**, 15368 (1999).  
 29. Z. R. Wasilewski, S. Fafard, J. P. McCaffrey, *J. Cryst. Growth* **201**, 1131 (1999).  
 30. J. P. McCaffrey et al., *J. Appl. Phys.* **88**, 2272 (2000).  
 31. M. Korkusinski, P. Hawrylak, in preparation.  
 32. A. Wojs, P. Hawrylak, S. Fafard, L. Jacak, *Phys. Rev. B* **54**, 5604 (1996).  
 33. M. Bayer, O. Stern, P. Hawrylak, S. Fafard, A. Forchel, *Nature* **405**, 923 (2000).  
 34. M. Bayer et al., data not shown.  
 35. This work has been carried out under the Canadian European Research Initiative on Nanostructures supported by the European Commission (IST-FET program); by the Institute for Microstructural Sciences, Canadian National Research Council (IMS NRC); and by the Canadian Natural Sciences and Engineering Research Council. The Würzburg group acknowledges support by the Deutsche Forschungsgemeinschaft, the U.S. Defense Advanced Research Projects Agency, and the State of Bavaria. M.K. thanks the IMS NRC for financial support; P.H. thanks the Alexander von Humboldt Foundation for support.

21 July 2000; accepted 4 December 2000

# A Lost-Wax Approach to Monodisperse Colloids and Their Crystals

Peng Jiang, Jane F. Bertone, Vicki L. Colvin\*

We report a nanoscale “lost-wax” method for forming colloids with size distributions around 5% and their corresponding colloidal crystals. Macroporous polymer templates are first prepared from a silica colloidal crystal. We then use the uniform and interconnected voids of the porous polymer to generate a wide variety of highly monodisperse inorganic, polymeric, and metallic solid and core-shell colloids, as well as hollow colloids with controllable shell thickness, as colloidal crystals. We can also uniformly deform the polymer template to alter colloidal shape and demonstrate the formation of elliptical particles with precisely controlled aspect ratios.

Monodisperse colloids have uniform physical and chemical properties that are useful for the quantitative evaluation of the optical, magnetic, electrokinetic, or adsorptive behavior of colloidal matter. In addition, highly uniform colloids offer superior properties for commercial applications ranging from magnetic recording to optical pigments (1). When sedimented, colloids with size distributions less than 5% can form three-dimensional (3D) periodic colloidal crystals. Existing strategies for preparing monodisperse colloids and nanoparticles generally manipulate

the chemistry of colloid formation (1, 2). Only silica and some polymer colloids can be routinely prepared with the narrow size distributions required for forming monolithic high-quality colloidal crystals (3). Unfortunately, these colloids do not exhibit the optical, nonlinear optical, or electro-optical functionality of other materials. In addition, although several methods have been developed to make colloidal crystals from silica and polymer colloids (4), colloidal crystallization is difficult for other denser colloids.

We report a physical rather than chemical strategy for forming virtually any colloid with size distributions of 5%. Rather than developing separate chemical methods for different materials, an alternative approach is to use high-quality colloidal crystals to create templates for the formation of a second gen-

Department of Chemistry, Center for Nanoscale Science and Technology, Rice University, Houston, TX 77005, USA.

\*To whom correspondence should be addressed. E-mail: colvin@rice.edu